



HAL
open science

Estimation of characteristic coagulation time based on Brownian coagulation theory and stability ratio modeling using electrokinetic measurements

Kevin Lachin, Nathalie Le Sauze, Nathalie Di Miceli Raimondi, Joelle Aubin,
Michel Cabassud, Christophe Gourdon

► **To cite this version:**

Kevin Lachin, Nathalie Le Sauze, Nathalie Di Miceli Raimondi, Joelle Aubin, Michel Cabassud, et al..
Estimation of characteristic coagulation time based on Brownian coagulation theory and stability ratio
modeling using electrokinetic measurements. *Chemical Engineering Journal*, 2019, 369, pp.818-827.
10.1016/j.cej.2019.03.130 . hal-02292121

HAL Id: hal-02292121

<https://hal.science/hal-02292121>

Submitted on 20 Sep 2019

HAL is a multi-disciplinary open access archive for the deposit and dissemination of scientific research documents, whether they are published or not. The documents may come from teaching and research institutions in France or abroad, or from public or private research centers.

L'archive ouverte pluridisciplinaire **HAL**, est destinée au dépôt et à la diffusion de documents scientifiques de niveau recherche, publiés ou non, émanant des établissements d'enseignement et de recherche français ou étrangers, des laboratoires publics ou privés.









Open Archive Toulouse Archive Ouverte

OATAO is an open access repository that collects the work of Toulouse researchers and makes it freely available over the web where possible

This is an author's version published in: <http://oatao.univ-toulouse.fr/24236>

Official URL: <https://doi.org/10.1016/j.cej.2019.03.130>

To cite this version:

Lachin, Kevin  and Le Sauze, Nathalie  and Di Miceli Raimondi, Nathalie  and Aubin, Joelle  and Cabassud, Michel  and Gourdon, Christophe  *Estimation of characteristic coagulation time based on Brownian coagulation theory and stability ratio modeling using electrokinetic measurements.* (2019) Chemical Engineering Journal, 369. 818-827. ISSN 1385-8947

Any correspondence concerning this service should be sent to the repository administrator: tech-oatao@listes-diff.inp-toulouse.fr

Estimation of characteristic coagulation time based on Brownian coagulation theory and stability ratio modeling using electrokinetic measurements

K. Lachin, N. Le Sauze, N. Di Miceli Raimondi*, J. Aubin, M. Cabassud, C. Gourdon

Laboratoire de Génie Chimique, Université de Toulouse, CNRS, INPT, UPS, Toulouse, France

HIGHLIGHTS

- The characteristic time of coagulation of colloidal suspensions is studied.
- The rate of coagulation is estimated using Brownian coagulation theory.
- The collision efficiency is taken into account through a stability ratio.
- Electrokinetic measurements are used to model the stability ratio.
- The method is applied to a latex: coagulation times and mixing times are compared.

ABSTRACT

Coagulation is a key process particularly in the field of polymer production. Controlling this phenomenon at industrial scale is a significant challenge because it is highly dependent on the operating conditions and the equipment used for the coagulation process. Poor control of coagulation may strongly affect the quality and the reproducibility of the final aggregates. In the objective of facilitating the choice of both adequate operating conditions and suitable devices for coagulation processes, this paper presents a method to estimate characteristic coagulation time of colloidal suspensions as a function of pH, ionic strength and volume fraction of particles. This method is based on Brownian coagulation theory, assuming very small initial particles. The collision efficiency is taken into account by the introduction of a stability ratio. This ratio is calculated using models that have been adjusted using electrokinetic measurements. The developed methodology is then applied to an industrial latex in order to estimate the operating conditions to fully destabilized the latex. Orders of magnitude of characteristic coagulation time are also obtained. Since perfect mixing of the colloidal suspension and the coagulant is necessary to obtain satisfactory aggregate properties, the characteristic coagulation time is compared with the mixing time for different mixing technologies, providing useful information for process design.

1. Introduction

Synthetic latexes are commonly used suspensions in polymer industries, and typically results from batch emulsion polymerization synthesis [1,2]. Depending on the end product to be manufactured, coagulation of the latex particles may be a desired process, typically occurring after polymerization, or it may be undesired, in which case it occurs during the polymerization process or other post-processing operations. However, regardless of the context, coagulation needs to be perfectly controlled to avoid quality and safety issues related to the Particle Size Distribution (PSD) and the morphology of the aggregates

[3].

Two main collision mechanisms can lead to coagulation. The first is orthokinetic coagulation in which case coagulation is controlled by the hydrodynamics in the reactor and industrially occurs in batch vessels. Consequently, significant literature on orthokinetic coagulation in batch tanks can be found [4–7]. When the particles are large enough, the fluid motion will have an impact on the trajectory of the particles forcing them to collide. However, another phenomenon can also intervene: Brownian motion will make the particles oscillate around their equilibrium position. In this case, the term perikinetic coagulation is used. This collision mechanism is generally predominant for particles in

* Corresponding author.

E-mail address: nathalie.raimondi@iut-tlse3.fr (N. Di Miceli Raimondi).

Nomenclature

a	Initial particle radius (m)
$[A^-]_s$	A^- number concentration per surface unit (m^{-2})
$[AH]_s$	AH number concentration per surface unit (m^{-2})
$\alpha_{H^+}^s$	Surface activity of the protons (m^{-2})
A	Hamaker constant (J)
c_{i0}	Molar concentration of the specie i ($mol.m^{-3}$)
d	particle diameter (m)
e	Elementary charge constant (C)
h	Interparticular distance (surface to surface) (m)
I	Ionic strength ($mol.m^{-3}$)
I_{init}	Initial ionic strength ($mol.m^{-3}$)
I_{lim}	Ionic strength beyond which the desorption is fully reached ($mol.m^{-3}$)
K_a	Surfactant dissociation constant (-)
$K_{a(acid)}$	Acid dissociation constant (-)
k_B	Boltzmann constant ($J.K^{-1}$)
k_{Br}	Brownian coagulation kernel ($m^3.s^{-1}$)
k_{Br}'	Brownian coagulation kernel including the stability ratio ($m^3.s^{-1}$)
m	Drag coefficient (-)
n	Bulk ion number density (m^{-3})
N	Particles number concentration (m^{-3})
N_A	Avogadro number (mol^{-1})
N_0	Initial particles number concentration (m^{-3})
t	Time (s)
T	Temperature (K)
t_c	Characteristic coagulation time (s)
t_m	Mixing time (s)

V_a	Attractive potential (J)
V_{acid}	Experimental volume of acid added to the latex (m^3)
V_{add}	Calculated volume of acid added to the latex (m^3)
V_{init}	Initial volume of the solution (m^3)
V_r	Electrostatic repulsive potential (J)
V_t	Total interaction potential (J)
W_{Br}	Brownian stability ratio (-)
x_z	Distance between the surface of the particle and the shear plane (m)
z	charge number (-)

Greek letters

ϵ_0	Vacuum permittivity ($F.m^{-1}$)
ϵ_r	Water relative permittivity (-)
Γ_{ion}	Surface density of chargeable sites due to the adsorbed ions (m^{-2})
Γ_{tot}	Total surface density of chargeable sites due to the surfactant (m^{-2})
κ	Debye-Huckel parameter (m^{-1})
μ	Dynamic viscosity (Pa.s)
μ_E	Electrophoretic mobility ($m^2.V^{-1}.s^{-1}$)
ϕ_0	Surface potential (V)
φ_0	Volume fraction (-)
σ_1	Surface charge density due to the chemical functions (m^{-2})
σ_2	Surface charge density at the surface of the particle in the diffuse layer (m^{-2})
σ_1'	Additional surface charge density (m^{-2})
ζ	Zeta potential (V)

the colloidal size range (between 1 nm and 1 μm) [8]. Melis et al. suggested a modified Péclet number (ratio of shear rate to particle diffusion rate) as a criterion to establish if coagulation is affected or not by hydrodynamics [9].

Beyond the hydrodynamic or Brownian motion which causes the particles to collide, their adhesion can only take place under favorable physicochemical conditions. Indeed, latexes are composed of colloidal particles, displaying charges on their surface either provided by chemical functions (monomer, surfactant...) or ions, which are adsorbed at the surface of the particles. These charges grant the metastability of latex. For most cases, coagulation does not occur naturally and must be triggered by a coagulant to modify the charge density at the surface of the particles. Among the different coagulants, salts and acids are widely used. A major challenge in coagulator design lies in physically contacting the coagulant and the colloidal suspension. Indeed, good mixing between both is required prior to coagulation in order to control the early stages of the coagulation process. Mixing should be relatively fast in order to avoid heterogeneities in coagulant concentration in the coagulator that may degrade the quality of the final product. Therefore understanding how a colloidal suspension evolves in the early stages of the coagulation process as a function of the operating conditions is essential to adequately design a coagulator. Population balances, eventually coupled with Navier-Stokes continuum equations, are generally used to predict Particle Size Distribution and coagulation time [10–17]. However, these approaches can be time-consuming and their reliability and genericity highly depends on the models used to describe the coagulation and breakage kernels, the hydrodynamics and the complex rheology of colloidal suspensions. In the present article, an approach using characteristic times is proposed to aid process design. A characteristic time is not directly related to the time to complete an operation but is relevant to the dynamics of a fundamental phenomenon. The approach of characteristic times is very useful to provide insight into the relative rate of basic phenomena (e.g. reaction vs.

mixing; advective transport vs. diffusive transport). Therefore, characteristic times are of great utility in chemical engineering for understanding and modeling processes, as well as equipment design and scale-up [18,19]. In the literature, characteristic times of orthokinetic coagulation can be obtained with simple models, which are a function of shear rate and initial particle size [20,21]. For Brownian coagulation, simple models exist to predict the time of coagulation but they assume fully destabilized colloidal suspensions. More realistic approaches should take into account partial destabilization and require the modeling of interparticulate forces that are complex to express as a function of the operating conditions.

The aim of the present paper is to present an original methodology for estimating the characteristic coagulation time of a latex suspension as a function of ionic strength, pH of the medium and solid volume fraction. Brownian coagulation theory is considered. The influence of the stability of the colloidal suspension is taken into account in the coagulation kernel, using electrophoretic mobility measurements to model this stability. The strength of this work is to propose an adequate experimental protocol and data analysis to lead to the modeling of the colloidal solution stability. The methodology is illustrated with an industrial latex coagulation stabilized by carboxylic acid surfactants, where the obtained characteristic times of coagulation at different operating conditions are finally compared with characteristic times of mixing in diverse technologies.

2. Theory

2.1. Interparticular interactions

2.1.1. DLVO theory

The simplest, yet widely used theory explaining colloidal stability is called DLVO theory and was simultaneously proposed by Derjarguin and Landau [22] and Verwey and Overbeek [23]. This theory stipulates

that the colloidal stability can be interpreted as a balance at the particle scale between the Van der Waals attractive forces and the electrostatic repulsive forces such that:

$$V_t = V_a + V_r \quad (1)$$

where V_t stands for the total potential energy of interaction between two particles, V_a the attractive potential energy and V_r the repulsive potential energy. A suspension is usually considered stable if the maximum value of V_t (the energy barrier) exceeds $15k_B T$ [24] where k_B is the Boltzmann constant and T the temperature. Despite its relative simplicity (some forces, such as solvation forces are here not taken into account), there has been successful use of this theory in the literature [25].

2.1.2. Van der Waals attractive forces

The literature distinguishes between two main approaches for calculating the Van der Waals attractive forces: the Lifschitz approach [26] and the Hamaker approach [27]. To be fully relevant, the Lifschitz approach requires the knowledge of optical properties of the materials considered over the complete electromagnetic spectrum, and these are available for only a restricted number of materials. In the case of polystyrene latex, examples of the application of this theory can be found in [28]. The Hamaker approach is more widely used. Whereas this approach does not take into account the retardation forces that can possibly be present, it approximates the Van der Waals attractive forces with an accuracy of about 10–20%, which is suitable for most cases [29]. The most widely used expression for V_a when considering two particles of same radius a is given by Eq. 2:

$$V_a = -\frac{Aa}{12h} \quad (2)$$

where h is the interparticulate distance and A the Hamaker constant. While it is an approximation of the full Hamaker expression, this formula can reasonably be used for h values when $h \ll a$ [30]. Theoretical expressions [31,32] allow the calculation of A in vacuum for a considered material, and tabulated values for Hamaker constants of polymer materials immersed in water can easily be found in literature. The order of magnitude for A for polymer materials is 10^{-20} J [33].

2.1.3. Electrostatic repulsive forces

When a particle is immersed in a liquid medium, a charge density can appear at its surface. This charge density can either be due to the dissociation of chemical functions located at the surface of the particle, or be related to the adsorption of some species like surfactants or ions. When the immersion medium contains dissolved electrolytes, this surface charge will generate an uneven ion and counter-ion distribution near the surface of the considered particle. This physical statement is at the core of the theory formulated by Gouy and Chapman [34–36] that was later modified by Stern [37] to formulate the theory of the electronic double layer.

When two colloidal particles approach, the recovery of their electronic layers will generate an electrostatic repulsive force, which can prevent particles from colliding if the repulsive force is strong enough. The electrostatic potential energy of a particle depends on a parameter, κ , also called Debye-Hückel parameter as shown by Eq. 3.

$$\kappa = \sqrt{\frac{2e2N_A I}{\epsilon_r \epsilon_0 k_B T}} \quad (3)$$

κ depends on the temperature T and the ionic strength I of the medium, which can be calculated from Eq. 4:

$$I = \frac{1}{2} \sum_i c_{i0} z_i^2 \quad (4)$$

κ is often introduced under its inverse form, κ^{-1} , which is called the Debye-Hückel length and is an essential parameter when studying colloidal interactions as it approximately quantifies the thickness of the

particle electronic atmosphere. The value κa is thus widely used in order to compare the range of repulsive forces to the radius of the considered particle. The knowledge of κ is of great use to calculate the repulsive potential. For identical spherical particles of radius a immersed in a symmetrical electrolyte of valence z , and assuming that κa is large enough ($\kappa a \gg 1$), it is possible to express the potential repulsive energy V_r such that [23,30]:

$$V_r = \frac{64\pi n k_B T}{\kappa^2} \gamma_0^2 \exp(-\kappa h) \quad (5)$$

$$\gamma_0 = \tanh\left(\frac{ze\phi_0}{4k_B T}\right) \quad (6)$$

where n denotes the bulk ion number density and ϕ_0 the surface potential.

2.1.4. Particle charge balance

As V_r depends on the surface potential of the particle ϕ_0 , it is essential to access this value. It can be obtained from a charge balance at the particle surface as follows. If we consider a colloidal particle, the chemical functions at its surface will grant a surface charge density σ_1 . When these chemical functions obey a dissociation equilibrium (for example acid-base equilibrium like it is the case of the studied latex), σ_1 will depend on the concentration of the species that intervene in the equilibrium and pH will thus have a significant impact on σ_1 . When considering particles stabilized by acid functions A^- (with an ion number concentration per surface unit $[A^-]_s$), σ_1 can be expressed as follows:

$$\sigma_1 = -e[A^-]_s \quad (7)$$

The dissociation constant K_a can be expressed as a function of $[A^-]_s$, $[AH]_s$ and the proton activity at the surface of the particle $a_{H^+}^s$ such that:

$$K_a = \frac{a_{H^+}^s [A^-]_s}{[AH]_s} \quad (8)$$

Using a Boltzmann equation, it is possible to express $a_{H^+}^s$ as a function of the surface potential ϕ_0 :

$$a_{H^+}^s = \exp\left(\frac{-e \cdot \phi_0}{k_B \cdot T}\right) 10^{-pH} \quad (9)$$

The total density of chargeable sites per surface area, assuming that only the acid function considered grants charges, can simply be expressed as:

$$\Gamma_{tot} = [A^-]_s + [AH]_s \quad (10)$$

Combining Eqs. 7–10, the following expression for σ_1 is obtained, being a function of the pH of the suspension and the surface potential of the considered particle ϕ_0 :

$$\sigma_1 = \frac{-e\Gamma_{tot}}{1 + \frac{10^{-pH}}{K_a} \exp\left(\frac{-e\phi_0}{k_B T}\right)} \quad (11)$$

The Poisson-Boltzmann equation relates the charge density granted by the counter-ions in the diffuse layer to the electrostatic repulsive potential. By integrating this charge density over distance, from the particle surface to infinity, it is possible to write a relationship between the electrostatic repulsive potential and the charge per surface unit in the diffuse layer. The surface charge density at the surface of the particle is σ_2 . For a symmetrical electrolyte, the following expression can be used:

$$\sigma_2 = -\frac{2\kappa k_B T \epsilon_r \epsilon_0}{ze} \left[\sinh\left(\frac{ze\phi_0}{2k_B T}\right) + \frac{2}{\kappa a} \tanh\left(\frac{ze\phi_0}{4k_B T}\right) \right] \quad (12)$$

Eq. 14, proposed by Loeb et al. [38] and later used in other studies [39], takes into account the surface curvature of the particle considered and is thus particularly suitable to the study of latex stability.

Using a simple charge balance, the following relation is then obtained:

$$\sigma_1 + \sigma_2 = 0 \quad (13)$$

By solving this balance, it is thus possible to calculate ϕ_0 as a function of the pH and the ionic strength (through the calculation of κ) of the medium. However, the total surface density of chargeable sites Γ_{tot} is unknown. The originality of the current work is to determine this data by comparing calculated electrophoretic mobilities μ_E , which depend on Γ_{tot} , and experimental values obtained at different pH and ionic strength conditions, as described in the following section.

2.2. Brownian coagulation theory

For small particles with a diameter less than a few hundred of nanometers, Brownian motion will cause the particles to move around their equilibrium position and will ultimately lead to particle collision and thus coagulation. Smoluchowski [40] was the first to theorize coagulation kinetics in analogy with chemical kinetics. When considering a monodisperse suspension of spherical particles, the following relation was proposed to describe the early stages of perikinetic coagulation:

$$\frac{dN}{dt} = -k_{Br}N^2 = \frac{4k_B T}{3\mu}N^2 \quad (14)$$

where k_{Br} is the Brownian coagulation kernel and N the concentration of particles in number. It is worth mentioning that this theory supposes that the collisions are binary, and thus is not valid for concentrated suspensions.

The kernel introduced above is strictly valid when all the collisions are efficient, that is to say leading to coagulation. However, this

situation is only valid when the suspension is fully destabilized, which means that the magnitude of repulsive forces is too low to prevent coagulation from occurring. In order to take into account the efficiency related to the physicochemical properties of the suspension, Fuchs [41] was the first to introduce the Brownian stability ratio, W_{Br} . The expression was further improved to take into account the attractive forces in the rapid coagulation regime and the hydrodynamic interactions, as given by Eq. 15 [30,42]:

$$W_{Br} = \frac{2a \int_0^{\infty} B(h) \cdot \frac{\exp\left(\frac{V_r}{k_B T}\right)}{(h+2a)^2} dh}{2a \int_0^{\infty} B(h) \cdot \frac{\exp\left(\frac{V_a}{k_B T}\right)}{(h+2a)^2} dh} \quad (15)$$

$$B(h) = \frac{6(h/a)^2 + 13(h/a) + 2}{6(h/a)^2 + 4(h/a)} \quad (16)$$

where h is the distance between two particles, and $B(h)$ a function taking the hydrodynamic interaction into account. W_{Br} can be considered as the inverse of a collision efficiency, which is related to the physico-chemistry of the medium. Its value ranges between 1 for totally destabilized suspensions and $+\infty$ for stable suspensions. By considering the DLVO theory (Eq. 1) and the expressions for V_a and V_r introduced by Eqs. 2 and 3, Ohshima [30] proposed an analytical expression for Eq. 15 to estimate W_{Br} :

$$W_{Br} = 1 + \frac{1}{2q_0} \sum_{m=1}^{\infty} \frac{1}{m!} \left(\frac{G\kappa a}{12}\right)^m K_0\left(\sqrt{\frac{A\kappa a m}{3k_B T}}\right) \quad (17)$$

$$q_0 = \frac{11}{8} \exp\left(\frac{A}{24k_B T}\right) E_1\left(\frac{A}{24k_B T}\right) - \frac{9}{8} \exp\left(\frac{A}{8k_B T}\right) E_1\left(\frac{A}{8k_B T}\right) \quad (18)$$

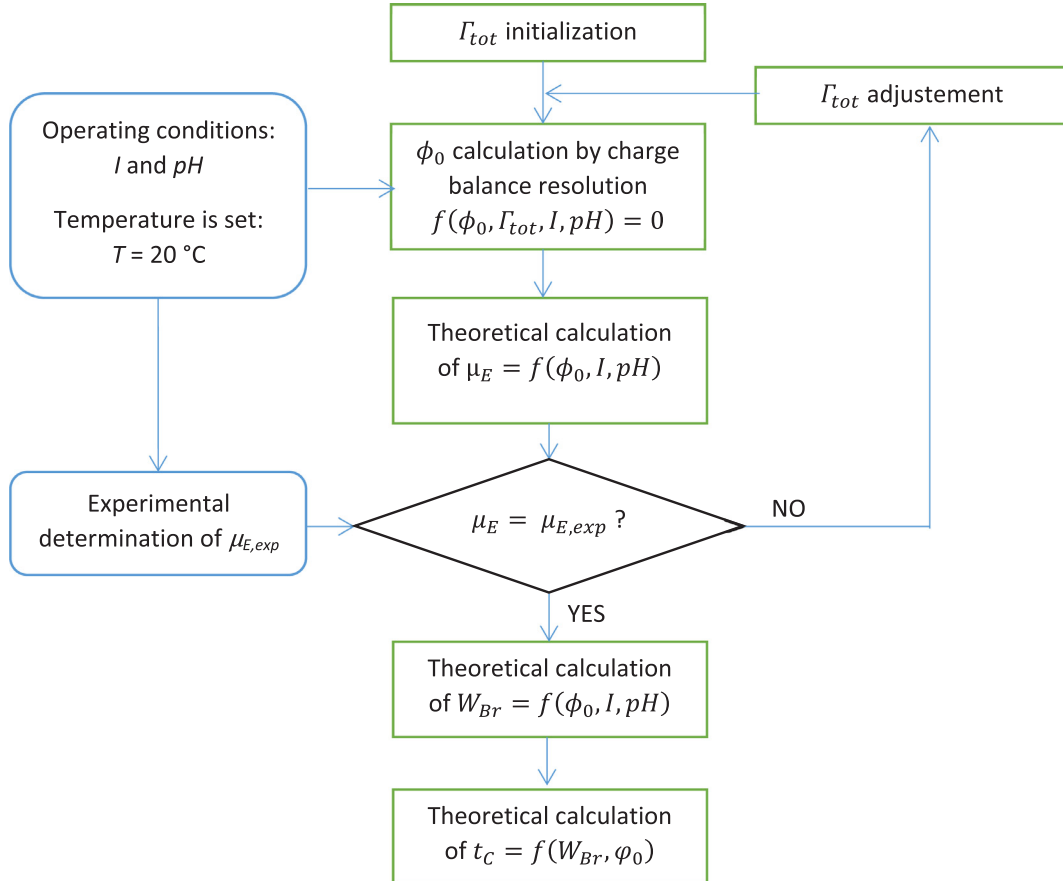


Fig. 1. Flowsheet describing the method to determine t_c .

Table 1
Summary of the model parameters.

Parameter type	Symbol	Value
Fixed	x_z	0.2 nm
	K_a	10^{-5}
	T	20 °C
Adjusted	Γ_0	—
Calculated	φ_0	Eq. 13
	ζ	Eq. 22
	μ_E	Eq. 23

$$G = \frac{384\pi(\gamma_0)2\varepsilon_r\varepsilon_0k_B T}{e2\kappa} \quad (19)$$

where E_1 is the 1st order exponential integral and K_0 the 0th order modified Bessel function of the second kind.

As a consequence, it is possible to express a new Brownian kinetic kernel taking into account the inter-particulate forces for suspensions that are not fully destabilized through the use of W_{Br} :

$$k'_{Br} = \frac{1}{W_{Br}} k_{Br} \quad (20)$$

Eq. 14 is analogous to second-order chemical reaction kinetics and can be used to estimate a Brownian characteristic coagulation time (here assimilated to a half-life time) expressed as follows:

$$t_c = \frac{1}{k'_{Br}N_0} = \frac{W_{Br}\pi\mu\alpha^3}{k_B T\varphi_0} \quad (21)$$

where N_0 is the initial number concentration of particles and φ_0 the volume fraction of the suspension ($\varphi_0 = N_0 \frac{4\pi a^3}{3}$). Due to the simplifications used to establish such a model, Eq. 20 should be considered qualitatively and not quantitatively; however, it can be of a great use to estimate whether a latex can be considered stable through time or not.

3. Materials and methods

3.1. Strategy

The strategy developed in this work to access the characteristic time of Brownian coagulation from pH and ionic strength values is summarised in Fig. 1. The surface potential ϕ_0 is estimated by solving the charge balance equation (Eqs. 11–13) using MATLAB with the FSOLVE function where the surface potential is taken as the variable. The theoretical and experimental determinations of the electrophoretic mobility are described in the next sections.

3.2. From surface potential ϕ_0 to theoretical electrophoretic mobility μ_E

The theoretical electrophoretic mobility can be calculated from the value of ϕ_0 . More precisely, the zeta potential is calculated for a given surface potential with Eq. 22, giving access to the corresponding electrophoretic mobility in Eq. 23.

$$\zeta = \frac{4k_B T}{ze} \cdot \arctanh \left[\exp(-\kappa x_z) \tanh \left(\frac{ze\phi_0}{4k_B T} \right) \right] \quad (22)$$

where x_z represents the distance between the shear plane and the surface of the particle. Eq. 22 is strictly valid for plane surfaces, however Behrens et al. [39] considered the precision of this equation satisfactory when ϕ_0 is estimated using Eq. 12, which takes the surface curvature into account. For this study, x_z is taken equal to 0.2 nm, which is a physical order of magnitude for this distance [24].

$$\mu_E = \frac{2k_B T \varepsilon_r \varepsilon_0}{3\mu e} \left(\frac{3e\zeta}{2k_B T} - \frac{\frac{3e\zeta}{k_B T} - \frac{6\ln(2)}{z} \left[1 - \exp\left(\frac{-ze\zeta}{k_B T}\right) \right]}{2 + \left[\frac{\exp\left(\frac{-ze\zeta}{2k_B T}\right)\kappa a}{1 + \frac{3m}{z^2}} \right]} \right) \quad (23)$$

m is the drag coefficient equal to 0.184 [43]. Eq. 23 is proposed by O'Brien and Hunter for $\kappa a \geq 30$ and $|\zeta| \leq 250$ mV. The modeling proposed in this study relies on equations strictly valid for symmetrical electrolytes. Even if a 1:2 electrolyte is added in the experiments introduced in this work, it has to be mentioned that in most of the experimental cases presented here, the ionic strength is mainly due to the symmetrical background electrolyte, explaining this choice. Other modeling approaches can however be found in the literature. Ohshima et al. [44] proposed an approximate expression of electrophoretic mobility in the case of symmetrical electrolytes successfully applied [42] and valid for $\kappa a \geq 10$, that however comes with a more complex analytical expression. Also, in the case of mixed solutions (1:1 and 2:1 or 1:1 and 3:1 electrolytes), Nishiyama et al. [45] proposed a modeling strategy from the surface potential to the electrophoretic mobility based on Ohshima approximations. As the electrolytes used in this study are 1:1 and 1:2, this approach was not considered here.

Table 1 summarises the parameters considered in this study. The surfactant used to stabilize the latex is a carboxylic acid with a dissociation constant K_a equal to 10^{-5} .

3.3. Electrophoretic mobility measurements

3.3.1. Set-up and coagulant

In order to measure the impact of both pH and I on the electrophoretic mobility measurements, acid titrations are performed on latex with different initial ionic strengths. Measurements are performed using a Malvern Nanosizer ZS[®] and a MPT-2 titrator is used to ensure reliable pH adjustment. pH is monitored using a Malvern pH-probe (SEN106). Each measurement is performed in a Malvern DTS1060 folded capillary cell. Industrially, pH-sensitive latex is often destabilized using sulfuric acid. For this reason, titrations are performed using H₂SO₄ at a concentration equal to 0.05 M. Measurements are performed from pH = 7.5 to pH = 1.5.

3.3.2. Latex

The latex used in this study is a core-shell PMMA/PABu copolymer, stabilized by a carboxylic acid surfactant. All the experiments are carried out using a suspension at initial concentration $1.375 \times 10^{-3}\%$ (w/w), obtained after initially diluting an industrial latex (33% w/w) using ultrapure water (Purelab[®] Option-Q). The volume-average radius of the latex particles is $a = 141$ nm ($d = 282$ nm), measured using a Malvern Nanosizer ZS[®]. The measured monomodal distribution is presented in Fig. 2.

Four samples of 12 mL are used for the study. With the use of KCl as a background electrolyte, the initial ionic strength of the suspension is adjusted at four different values: 0 mM, 10 mM, 50 mM and 100 mM.

3.4. Ionic strength variation through the titration

While adding H₂SO₄ to the latex, both the dilution and the addition of an electrolyte will change the ionic strength of the suspension. For a volume of acid added V_{add} , the ionic strength, I , can be expressed as follows:

$$I = I_{acid} + I_{init} \frac{V_{init}}{V_{init} + V_{add}} \quad (24)$$

H₂SO₄ is a dibasic acid ($pK_{a,1} = -3$, $pK_{a,2} = 1.9$). Since the pH ranges from 1.5 to 7.5, only the weakest acidity is taken into account in order to propose an expression of V_{add} and I_{acid} as a function of the pH.

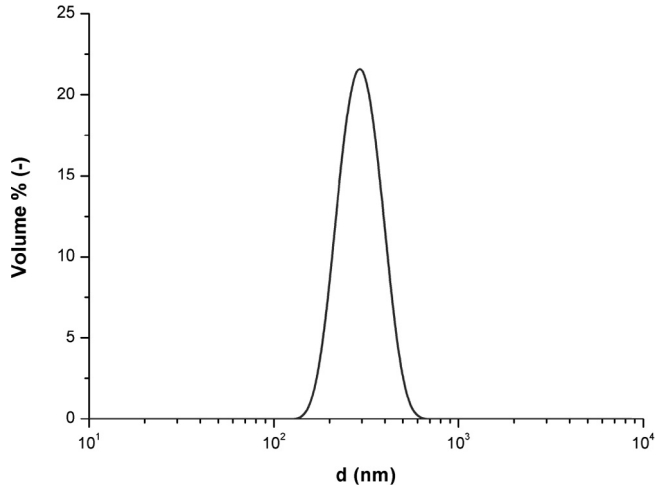


Fig. 2. Particle size distribution of the initial latex obtained with Nanosizer ZS[®].

Using a straightforward balance, it is possible to write the following relations to calculate I_{acid} and V_{add} :

$$I_{acid} = \frac{1}{2} \left(10^{-pH} + 4 \frac{10^{-pH}}{2 + \frac{10^{-pH}}{10^{-pK_a(acid)}}} + \frac{10^{-pH}}{1 + 2 \frac{10^{-pK_a(acid)}}{10^{-pH}}} \right) \quad (25)$$

$$V_{add} = \frac{V_{init} 10^{-pH}}{2[H_2SO_4] - \frac{[H_2SO_4]}{1 + 10^{-pK_a(acid)+pH}} - 10^{-pH}} \quad (26)$$

A comparison between the calculated V_{add} and experimental V_{acid} (given by the NanoZS software) for the titration at $I_{init} = 10$ mM is presented in Table 2. The results show good agreement and allow to better calculate I , and thus κ .

4. Results

4.1. Determination of Γ_{tot}

The model introduced earlier is firstly used in order to adjust Γ_{tot} , using the titration performed at I_{init} equal to 100 mM. Good agreement between experimental and theoretical results is obtained for $\Gamma_{tot} = 0.15 \text{ nm}^{-2}$, with a maximal relative difference between the theoretical and experimental electrophoretic mobilities of less than 1%. The comparison between the theoretical and experimental results can be seen in Fig. 3.

The adjusted model (Model 1) is then used to predict the evolution of the theoretical electrophoretic mobility with pH for the four ionic strengths studied experimentally ($I_{init} = 0, 10, 50, 100$ mM). The results are presented in Fig. 4.

At the highest ionic strengths studied (50 and 100 mM), the model and the experimental results are in good agreement over the whole pH range. For $I_{init} = 0$ mM and 10 mM, however, the model clearly fails at representing the electrophoretic mobility, particularly at low pH values ($pH < 4$). The model supposes that all the charges are brought by the carboxylic surfactant. Below $pH = 3$, almost all the surfactant molecules are thus in their acid form, i.e. without charges, and in this case the electrophoretic mobility should be null. However, especially at low ionic strength, the mobility is far from being null, which means that other species are very likely to be present on the surface of the particles. As a consequence, the theoretical model needs to be corrected to take into account this experimental fact.

4.2. Modification of the charge balance solved

To prepare the latex, the polymerization is triggered using sodium

formaldehyde sulfoxylate. In an aqueous medium, hydroxymethanesulfonate ions will thus be present and in large majority compared with the other ionic species composing the latex. These ions are known to be unstable and to generate sulfoxylate ions in acidic mediums. As the ionic strength is increasing, these adsorbed ions will desorb further from the surface, in analogy with the desorption of ionic species in soils while increasing the ionic strength [46]. Several studies [42,45,47] compute the adsorbed charge density using a Stern layer model. However, this approach needs data (notably the ion bulk concentration) that is not given by the industrial latex provider. For this reason, a more straightforward model is used in this study.

The experimental results presented in Fig. 4 show that for $I_{init} = 100$ mM the results seem to be independent of the presence of an additional surface charge since the experimental and the theoretical results are in good agreement. However, they are slightly dependent for $I_{init} = 50$ mM since the model slightly underestimates the electrophoretic mobility for pH values lower than 2.5. σ_1 denotes this additional surface charge. Since no further data is provided on the possible desorption mechanism, the following expression, which assumes linear desorption with increasing ionic strength, is taken:

$$\sigma_1 = -e\Gamma_{ion} \frac{I_{lim} - I}{I_{lim}} \quad (27)$$

I_{lim} stands for the ionic strength value beyond which the desorption is totally achieved and is chosen equal to 70 mM (order of magnitude for which the second surface charge seems to be absent). Eq. 27 is considered for $I < I_{lim}$. If this is not the case, σ_1 is set to 0. The following balance is thus solved:

$$\sigma_1 + \sigma_1 + \sigma_2 = 0 \quad (28)$$

By adjusting Γ_{ion} to 0.03 nm^{-2} , the results given in Fig. 5 are obtained. At the lowest pH, it can clearly be observed that the behavior observed with this model (Model 2) is in better agreement with the experimental results. However, for $I_{init} = 0$ mM, a significant difference between the model and the experiments for pH values ranging from 2.5 to 5 is observed. This discrepancy can be interpreted as a limitation of the O'Brien and Hunter approximation at these pH values. Indeed, as mentioned before, Eq. 23 is proposed for $\kappa a \geq 30$ and $|\zeta| \leq 250$ mV. These conditions are fulfilled in the present study except for $I_{init} = 0$ mM and $pH > 2.4$.

For $I_{init} = 10$ mM, the model deviates from the experimental data considerably for $pH > 5$ due to the increase in mobility granted by the ion adsorption at low ionic strength. As the sulfoxylate ions appear in the acidic medium, at the highest pH, the effect of its adsorption at the particle surface on the charge balance should not be taken into account. This discrepancy therefore confirms that the extra surface charge is due to the presence of sulfoxylate ions.

The agreement of the model with ion adsorption (Model 2) with the experimental data was checked calculating the root-mean-square deviation (RMSD, Eq. 29) given in Table 3.

$$RMSD = \sqrt{\frac{1}{N} \sum_{i=1}^N (\mu_E - \mu_{E,exp})^2} \quad (29)$$

It can be seen that except in the case $I_{init} = 10$ mM, the deviation is lower using Model 2, confirming an improved agreement of the model as observed visually.

Table 2

Comparison of experimental and calculated V_{add} .

pH (-)	Experimental V_{add} (mL)	Calculated V_{add} (mL)
1.66	4.67	5.34
1.76	3.38	3.69
2.27	0.776	0.786
2.72	0.272	0.247

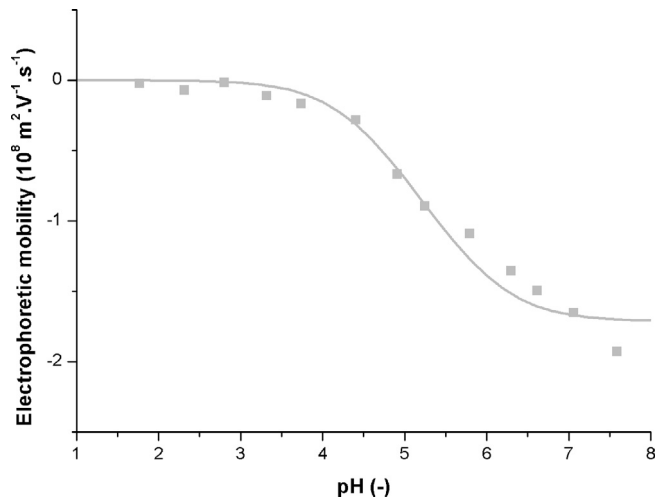


Fig. 3. Comparison between experimental (dots) and calculated (line) electrophoretic mobilities for $I_{init} = 100$ mM.

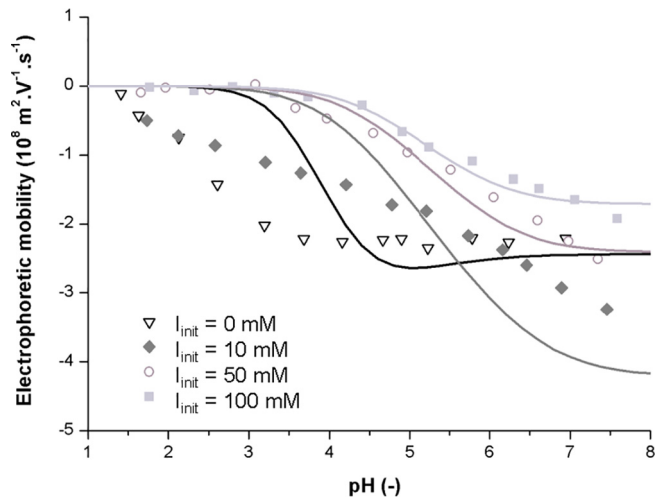


Fig. 4. Comparison between experimental (dots) and calculated (line) electrophoretic mobilities for $I_{init} = 0, 10, 50$ and 100 mM.

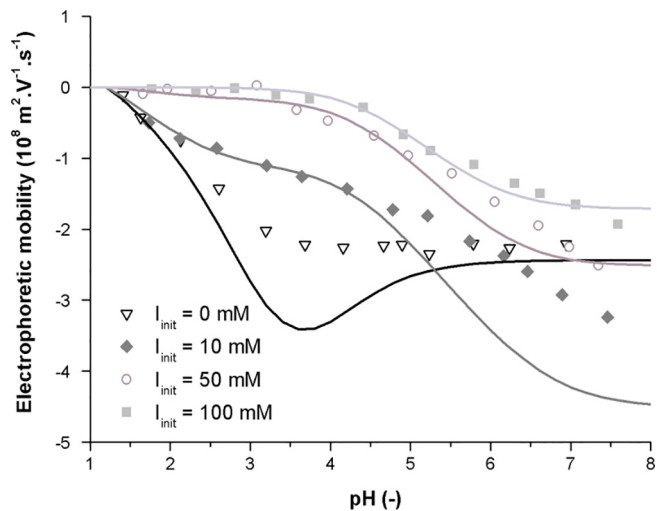


Fig. 5. Comparison between the experimental electrophoretic mobility (dots) and the adjusted calculated electrophoretic mobility (line) for $I_{init} = 0, 10, 50$ and 100 mM.

Table 3
RMSD calculations.

	RMSD(Model 1) ($m^2.V^{-1}.s^{-1}$)	RMSD(Model 2) ($m^2.V^{-1}.s^{-1}$)
$I_{init} = 0$ mM	7.76E-09	5.96E-09
$I_{init} = 10$ mM	7.83E-09	7.53E-09
$I_{init} = 50$ mM	1.77E-09	2.02E-09
$I_{init} = 100$ mM	1.05E-09	1.05E-09

Despite these limitations, the model reproduces the experimental electrophoretic mobility trends fairly well and is therefore used to estimate the surface potential as a function of pH and I . Indeed, for the purpose of developing a coagulation process (including the determination of optimal residence times, stirring characteristics etc.), the conditions where the model of electrophoretic mobility does not fit with the experimental data ($I_{init} = 0$ mM, $pH > 2.4$; $I_{init} = 10$ mM, $pH > 5$) should not be considered. It will be seen in the next section that characteristic coagulation times that are higher than 1000 s are estimated under these conditions, signifying that the suspension is only slightly destabilized.

4.3. Estimation of W_{Br} using the surface potential model

The optimized surface potential model obtained can be used in the analytical W_{Br} expression proposed by Ohshima. The value chosen for the Hamaker constant, A , is 10^{-20} J, which is a common order of magnitude for polymers (Ottewill [33] proposes $A = 1.05 \cdot 10^{-20}$ J for PMMA, and $A = 0.95 \cdot 10^{-20}$ J for PS). Fig. 6 represents the evolution of $\log(W_{Br})$ as a function of pH for different initial ionic strengths (0, 10, 50 and 100 mM). The model considers that pH is adjusted using sulfuric acid and takes into account the variation in ionic strength introduced by the addition of the acid and its dissociation. As mentioned before, when W_{Br} equals 1 ($\log W_{Br} = 0$), the colloidal suspension is fully destabilized. As expected, Fig. 6 shows that the stability of the studied latex decreases with the pH. Moreover, it is observed that the maximum pH required to obtain full destabilization increases with the initial ionic strength of the solution. This is due to the fact that the presence of positive charges in the salt weakens the surface potential of the particles, thereby reducing the repulsive potential energy. Therefore, destabilization is obtained with a lower amount of acid in the presence of salt.

While these calculated stability ratios can be used for further kinetic modeling, it is also possible to extract very practical information for the

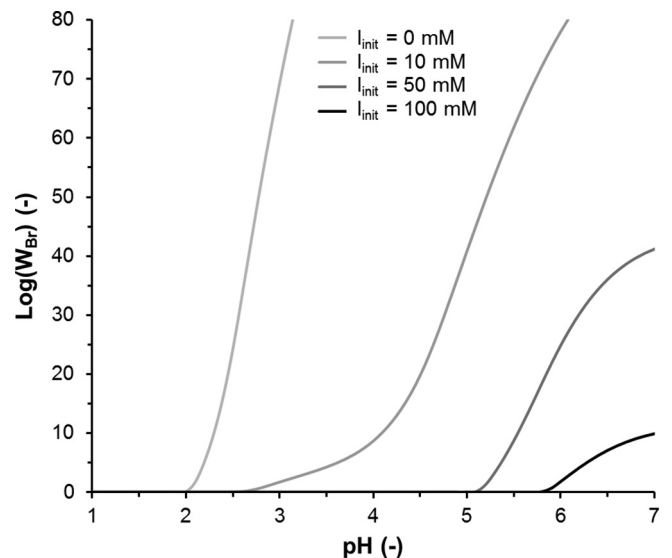


Fig. 6. $\log(W_{Br})$ as a function of pH for $I_{init} = 0, 10, 50$ and 100 mM.

experimenter. As we can see in Fig. 6, it is possible to obtain for a specific initial ionic strength the pH at which the suspension is fully destabilized. By representing this data on a master curve as presented in Fig. 7, it is possible for the experimenter to identify the minimum pH-value to be reached to ensure full destabilization at a given value of I_{init} . This information can be of great use if the objective is not to obtain specific W_{Br} values but simply to ensure full latex destabilization.

4.4. Coagulation characteristic time vs. mixing time

Using Eq. 21, it is possible to convert the values of W_{Br} into Brownian coagulation times. The results are presented in Fig. 8. As Eq. 21 depends on the volume fraction of the suspension φ_0 , the coagulation times are presented under the form $t_c \varphi_0$, which allows the calculation of the coagulation time over a wide range of φ_0 . Eq. 21 is obtained assuming the collisions between particles are binary, which is no longer the case at high volume fractions: Fig. 8 can therefore be reasonably used for φ_0 values that are lower than 0.01 [48]. At higher volume fractions, as multiple collisions can occur simultaneously, t_c is likely to be lower than that predicted by the proposed model. Depending on the physicochemical properties of the medium and the volume fraction of the suspension considered, the evolution of the coagulation time versus I and pH represents an interesting tool for an experimenter who requires information about the stability of the considered suspension in a more practical way than the stability ratio calculation. It is also interesting to see that for this specific latex, even considering a very low initial ionic strength, the coagulation time is minimal for pH values ≤ 1.8 , thus indicating that the suspension is fully destabilized regardless of the background electrolyte concentration. This information can be very useful for studying coagulation when full destabilization is most of the time desired. The methodology developed in this paper is thus useful for a scientist who wants to estimate the lifetime of a specific latex as a function of the physicochemical properties of the medium and the conditions ensuring full latex destabilization.

The knowledge of the characteristic time of the coagulation process can be of great help for engineers. Indeed, such a methodology can be used to wisely choose the experimental conditions (pH, ionic strength and volume fraction) and the design of the coagulator so that the characteristic time of coagulation is greater than the mixing time, thus ensuring reproducible experiments and good quality products. Indeed, poor mixing of the colloidal suspension and the coagulant may cause zones with high concentration of coagulant, leading to very fast particle coagulation and thus degrading the global morphology of the final aggregates and product quality. Fig. 8 shows the orders of magnitude of mixing times in different mixing devices. For stirred tanks, mixing time ranges from few seconds (for the mixing in turbulent flow regime of non-viscous fluids using effective stirrer technologies and baffles) to several minutes (particularly when the viscosities of the fluids to mix are very different) [49–53]. Although stirred tanks are the most widely used technology to carry out coagulation processes at industrial scale, experiments of coagulation in Taylor-Couette reactors are very often carried out for data acquisition. Indeed, these reactors generally provide homogeneous shear rate fields in the fluids (except close to the walls where edge effects appear) and so the modeling of the coagulation mechanism is simplified. Mixing times observed in Taylor flow devices range from 2 to 60 s [54]. Tubular reactors in the laminar flow regime, which favors the formation of spherical aggregates, are also used [55–60]. However, the laminar flow regime typically does not provide effective mixing and a mixing device should be used before the coagulator to mix the colloidal suspension and the coagulant. Intensified mixing technologies – predominantly continuous and miniaturized reactors – have also emerged over the last decades and provide very short mixing time as represented in Fig. 8 [61,62].

As for example, a suspension of the studied latex at $pH = 3$ and $I_{\text{init}} = 10$ mM will have a $t_c \varphi_0$ value equal to 0.1 s. If we consider a volume fraction of 0.01, the Brownian coagulation time of the latex will

be equal to 10 s. In this case, it is very likely that performing coagulation in a stirred tank may lead to poor PSD control as it corresponds to the order of magnitude of mixing time in very efficient stirred tanks. On the other hand, if the volume fraction of the suspension is 0.0002, the Brownian coagulation time equals 500 s, which is greater than conventional mixing times expected in stirred tanks. It is thus reasonable to perform coagulation in this type of device under these conditions.

5. Conclusion

Using theoretical considerations related to the Brownian kinetics of coagulation and the short-range interactions between particles, this paper presents an original methodology based on electrophoretic mobility measurements to ultimately estimate a characteristic coagulation time as a function of the ionic strength and the pH of the medium considered. The methodology is applicable to colloidal suspensions with very small initial particles (with diameters less than a few hundred nanometers) where coagulation is initiated by Brownian motion. The methodology is illustrated with an industrial latex that has a pH-sensitive stability. Whilst difficulties were encountered in modeling the electrophoretic mobility due to the probable presence of adsorbed ions at the surface of the particles, the electrophoretic model proposed reproduces the experimental trends relatively well, thereby suggesting that both the modeling approach and the estimation of the surface potential are sound. The charge model was then used to calculate the total interaction potential and ultimately the Brownian stability ratio and the Brownian coagulation time as a function of the pH and the initial ionic strength of the medium. This was performed assuming DLVO theory.

The overall methodology presented provides a tool for scientists providing a simple means to estimate the time required to obtain an observable coagulated state of a colloidal suspension as a function of the physicochemical conditions of the medium and the volume fraction of the particles. For engineers, knowledge of characteristic times is necessary to adequately choose the experimental conditions and the equipment to obtain an effective coagulation process. For industrial coagulation, it is necessary to perform the process without mixing limitations (between the coagulant and the colloidal suspension) in order to obtain aggregates of desired and constant quality. For the purpose of data acquisition, it is also important that mixing time is shorter than the characteristic coagulation time in order to avoid fouling of the reactor and to obtain a reliable estimation of coagulation kernels, as well as reproducible experiments.

Acknowledgement

This work was supported by the French National Research Agency (ANR) in the framework of the Scale-Up project (ANR-12-RMNP-0016).

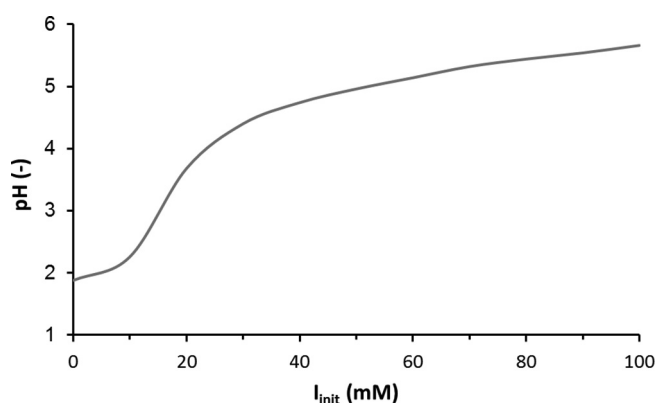


Fig. 7. pH vs. I_{init} to fully destabilize the latex.

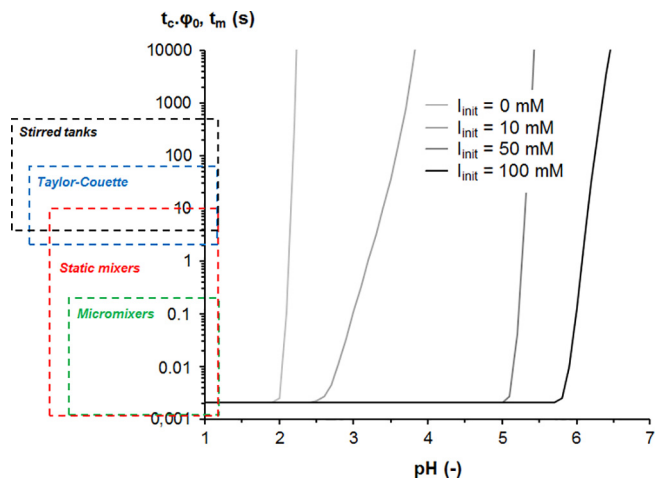


Fig. 8. Evolution of t_{c,ϕ_0} with pH for different I_{init} values. Comparison with mixing times t_m in different technologies.

References

[1] G.G. Odian, Principles of Polymerization, fourth ed., Wiley-Interscience, Hoboken, NJ, 2004.

[2] R.C. Elgebrandt, J.A. Romagnoli, D.F. Fletcher, V.G. Gomes, R.G. Gilbert, Analysis of shear-induced coagulation in an emulsion polymerisation reactor using computational fluid dynamics, *Chem. Eng. Sci.* 60 (2005) 2005–2015, <https://doi.org/10.1016/j.ces.2004.12.010>.

[3] N. Furukawa, W. Okada, Analysis of the coagulation rate of MBS (methylmethacrylate-butadiene-styrene) polymer latex and strength of coagula, *Adv. Powder Technol.* 5 (1994) 161–175.

[4] P.T.L. Koh, J.R.G. Andrews, P.H.T. Uhlherr, Flocculation in stirred tanks, *Chem. Eng. Sci.* 39 (1984) 975–985.

[5] De Boer, Coagulation in turbulent flow: part I, *Inst. Chem. Eng.* 67 (1989) 301–307.

[6] M. Soos, A.S. Moussa, L. Ehrl, J. Sefcik, H. Wu, M. Morbidelli, Effect of shear rate on aggregate size and morphology investigated under turbulent conditions in stirred tank, *J. Colloid Interface Sci.* 319 (2008) 577–589.

[7] T. Sugimoto, M. Kobayashi, Y. Adachi, The effect of double layer repulsion on the rate of turbulent and Brownian aggregation: experimental consideration, *Colloids Surf. Physicochem. Eng. Asp.* 443 (2014) 418–424, <https://doi.org/10.1016/j.colsurfa.2013.12.002>.

[8] C.-J. Chin, S. Yiacoymi, C. Tsouris, Shear-induced flocculation of colloidal particles in stirred tanks, *J. Colloid Interface Sci.* 206 (1998) 532–545, <https://doi.org/10.1006/jcis.1998.5737>.

[9] S. Melis, M. Verduyn, G. Storti, M. Morbidelli, J. Baldyga, Effect of fluid motion on the aggregation of small particles subject to interaction forces, *AIChE J.* 45 (1999) 1383–1393.

[10] D.L. Marchisio, J.T. Pikturna, R.O. Fox, R.D. Vigil, A.A. Barresi, Quadrature method of moments for population-balance equations, *AIChE J.* 49 (2003) 1266–1276.

[11] L. Wang, R.D. Vigil, R.O. Fox, CFD simulation of shear-induced aggregation and breakage in turbulent Taylor-Couette flow, *J. Colloid Interface Sci.* 285 (2005) 167–178, <https://doi.org/10.1016/j.jcis.2004.10.075>.

[12] J. Pohn, Scale-Up of Latex Reactors and Coagulators: A Combined CFD-PBE Approach, Queen's University, 2012.

[13] A. Falola, A. Borissova, X.Z. Wang, Extended method of moment for general population balance models including size dependent growth rate, aggregation and breakage kernels, *Comput. Chem. Eng.* 56 (2013) 1–11, <https://doi.org/10.1016/j.compchemeng.2013.04.017>.

[14] H. Zhao, C. Zheng, A population balance-Monte Carlo method for particle coagulation in spatially inhomogeneous systems, *Comput. Fluids* 71 (2013) 196–207, <https://doi.org/10.1016/j.compfluid.2012.09.025>.

[15] R.I. Jeldres, F. Concha, P.G. Toledo, Population balance modelling of particle flocculation with attention to aggregate restructuring and permeability, *Adv. Colloid Interface Sci.* 224 (2015) 62–71, <https://doi.org/10.1016/j.cis.2015.07.009>.

[16] M. Vlieghe, C. Coufort-Saudejaud, A. Liné, C. Frances, QMOM-based population balance model involving a fractal dimension for the flocculation of latex particles, *Chem. Eng. Sci.* 155 (2016) 65–82, <https://doi.org/10.1016/j.ces.2016.07.044>.

[17] A. Passalacqua, F. Laurent, E. Madadi-Kandjani, J.C. Heylmun, R.O. Fox, An open-source quadrature-based population balance solver for OpenFOAM, *Chem. Eng. Sci.* 176 (2018) 306–318, <https://doi.org/10.1016/j.ces.2017.10.043>.

[18] J.-M. Commenge, L. Falk, Methodological framework for choice of intensified equipment and development of innovative technologies, *Chem. Eng. Process. Process Intensif.* 84 (2014) 109–127, <https://doi.org/10.1016/j.cep.2014.03.001>.

[19] J. Aubin, J.-M. Commenge, L. Falk, L. Prat, Process Intensification by miniaturization, in: M. Poux, P. Cognet, C. Gourdon (Eds.), *Green Process Eng. Concepts Ind. Appl. Science Publishers (CRC Press/Taylor & Francis Group)*, 2015, pp. 77–108.

[20] F.E. Torres, W.B. Russel, W.R. Schowalter, Flocc structure and growth kinetics for

rapid shear coagulation of polystyrene colloids, *J. Colloid Interface Sci.* 142 (1991) 554–574.

[21] L.G. Bremer, P. Walstra, T. van Vliet, Estimations of the aggregation time of various colloidal systems, *Colloids Surf. Physicochem. Eng. Asp.* 99 (1995) 121–127.

[22] B. Derjaguin, L. Landau, Theory of the stability of strongly charged lyophobic sols and of the adhesion of strongly charged particles in solution of electrolytes, *Acta Physicochim. URSS* 14 (1941) 633.

[23] E.J. Verwey, J.T. Overbeek, *Theory of the Stability of Lyophobic Colloids*, Elsevier, Eindhoven, 1948.

[24] B. Cabane, *Chapitre 2: La stabilité colloïdale des latex*, *Latex Synth. Tec & Doc*, Lavoisier, 2006.

[25] M. Fortuny, C. Graillat, T. McKenna, Coagulation of anionically stabilized polymer particles, *Ind. Eng. Chem. Res.* 43 (2004) 7210–7219.

[26] E.M. Lifshitz, The theory of molecular attractive forces between solids, *Sov. Phys. JETP* 2 (1956) 73–83.

[27] H.C. Hamaker, The London-Van der Waals attraction between spherical particles, *Physica* 4 (1937) 1058–1072.

[28] M. Elzbiaciak-Wodka, M.N. Popescu, F.J.M. Ruiz-Cabello, G. Trefalt, P. Maroni, M. Borkovec, Measurements of dispersion forces between colloidal latex particles with the atomic force microscope and comparison with Lifshitz theory, *J. Chem. Phys.* 140 (2014) 104906, <https://doi.org/10.1063/1.4867541>.

[29] T.F. Tadros, *Colloid Stability: The Role of Surface Forces*, Wiley-VCH Verlag, Weinheim, 2007.

[30] H. Ohshima, Approximate analytic expression for the stability ratio of colloidal dispersions, *Colloid Polym. Sci.* 292 (2014) 2269–2274, <https://doi.org/10.1007/s00396-014-3257-1>.

[31] J. Visser, On Hamaker constants: a comparison between Hamaker constants and Lifshitz - Van der Waals constants, *Adv. Colloid Interface Sci.* 3 (1972) 331–363.

[32] J. Israelachvili, *Intermolecular and Surface Forces*, Academic Press, 1992.

[33] R. Ottewill, Chapter 3 - stabilization of polymer colloid dispersions, *Emuls. Polym. Emuls. Polym.* Wiley, Guildford, 1997, pp. 59–121.

[34] M. Gouy, Sur la constitution de la charge électrique a la surface d'un électrolyte, *J. Phys. Theor. Appl.* 9 (1910) 457–468.

[35] M. Gouy, *Ann. Phys.* (1917).

[36] D.L. Chapman, A contribution to the theory of electrocapillarity, *Philos. Mag. Ser. 6* (25) (1913) 475–481.

[37] O. Stern, Zur theorie der elektrolytischen doppelschicht, *Z. Elektrochem. Angew. Phys. Chem.* 30 (1924) 508–516.

[38] A.L. Loeb, J.Th G. Overbeek, P.H. Wiersema, *The Electrical Double Layer Around a Spherical Colloid*, The M.I.T. Press, Cambridge, Massachusetts, 1961.

[39] S.H. Behrens, D.I. Christl, R. Emmerzael, P. Schurtenberger, M. Borkovec, Charging and aggregation properties of carboxyl latex particles: experiments versus DLVO Theory, *Langmuir* 16 (2000) 2566–2575.

[40] M. Smoluchowski, Drei vortrage uber diffusion, Brownsche molekularbewegung und koagulation von kolloidteilchen, *Phys. Z. Sowjetunion.* 17 (1916) 557–599.

[41] N. Fuchs, Uber die stabilitat und aufladung der aerosole, *Z. Phys.* 89 (1934) 736–743.

[42] M. Kobayashi, S. Yuki, Y. Adachi, Effect of anionic surfactants on the stability ratio and electrophoretic mobility of colloidal hematite particles, *Colloids Surf. Physicochem. Eng. Asp.* 510 (2016) 190–197, <https://doi.org/10.1016/j.colsurfa.2016.07.063>.

[43] R.W. O'Brien, R.J. Hunter, The electrophoretic mobility of large colloidal particles, *Can. J. Chem.* 59 (1981) 1878–1887.

[44] H. Ohshima, T.W. Healy, L.R. White, Approximate analytic expressions for the electrophoretic mobility of spherical colloidal particles and the conductivity of their dilute suspensions, *J. Chem. Soc. Faraday Trans. 2* (79) (1983) 1613, <https://doi.org/10.1039/f29837901613>.

[45] M. Nishiya, T. Sugimoto, M. Kobayashi, Electrophoretic mobility of carboxyl latex particles in the mixed solution of 1:1 and 2:1 electrolytes or 1:1 and 3:1 electrolytes: experiments and modeling, *Colloids Surf. Physicochem. Eng. Asp.* 504 (2016) 219–227, <https://doi.org/10.1016/j.colsurfa.2016.05.045>.

[46] R. Naidu, N.S. Bolan, R.S. Kookana, K.G. Tiller, Ionic-strength and pH effects on the sorption of cadmium and the surface charge of soils, *Eur. J. Soil Sci.* 45 (1994) 419–429.

[47] A. Hakim, M. Nishiya, M. Kobayashi, Charge reversal of sulfate latex induced by hydrophobic counterion: effects of surface charge density, *Colloid Polym. Sci.* 294 (2016) 1671–1678, <https://doi.org/10.1007/s00396-016-3931-6>.

[48] M. Lattuada, P. Sandkühler, H. Wu, J. Sefcik, M. Morbidelli, Aggregation kinetics of polymer colloids in reaction limited regime: experiments and simulations, *Adv. Colloid Interface Sci.* 103 (2003) 33–56.

[49] K.W. Norwood, A.B. Metzner, Flow patterns and mixing rates in agitated vessels, *AIChE J.* 6 (1960) 432–437.

[50] I. Bouwmans, *The Blending of Liquids in Stirred Vessels*, Delft Univ. Press, Delft, 1992.

[51] M. Kraume, Mixing times in stirred suspensions, *Chem. Eng. Technol.* 15 (1992) 313–318.

[52] W.-M. Lu, H.-Z. Wu, M.-Y. Ju, Effects of baffle design on the liquid mixing in an aerated stirred tank with standard Rushton turbine impellers, *Chem. Eng. Sci.* 52 (1997) 3843–3851.

[53] I. Houcine, E. Plasari, R. David, Effects of the stirred tank's design on power consumption and mixing time in liquid phase, *Chem. Eng. Technol. Ind. Chem.-Plant Equip.-Process Eng.-Biotechnol.* 23 (2000) 605–613.

[54] A. Racina, Z. Liu, M. Kind, *Mixing in Taylor-Couette Flow*, in: H. Bockhorn, D. Mewes, W. Peukert, H.-J. Warnecke (Eds.), *Micro Macro Mix. Anal. Simul. Numer. Calc.* Springer Berlin Heidelberg, Berlin, Heidelberg, 2010, pp. 125–139, https://doi.org/10.1007/978-3-642-04549-3_8.

- [55] K. Higashitani, S. Miyafusa, T. Matsuda, Y. Matsuno, Axial change of total particle concentration in Poiseuille flow, *J. Colloid Interface Sci.* 77 (1980) 21–28.
- [56] J. Gregory, Flocculation in laminar tube flow, *Chem. Eng. Sci.* 36 (1981) 1789–1794.
- [57] I.C. Tse, K. Swetland, M.L. Weber-Shirk, L.W. Lion, Fluid shear influences on the performance of hydraulic flocculation systems, *Water Res.* 45 (2011) 5412–5418, <https://doi.org/10.1016/j.watres.2011.07.040>.
- [58] G. Farid Vaezi, R.S. Sanders, J.H. Masliyah, Flocculation kinetics and aggregate structure of kaolinite mixtures in laminar tube flow, *J. Colloid Interface Sci.* 355 (2011) 96–105, <https://doi.org/10.1016/j.jcis.2010.11.068>.
- [59] K. Lachin, N. Le Sauze, N. Di Miceli Raimondi, J. Aubin, C. Gourdon, M. Cabassud, Aggregation and breakup of acrylic latex particles inside millimetric scale reactors, *Chem. Eng. Process. Process Intensif.* 113 (2017) 65–73, <https://doi.org/10.1016/j.cep.2016.09.021>.
- [60] K. Lachin, N. Le Sauze, N. Di Miceli Raimondi, J. Aubin, D.F. Fletcher, M. Cabassud, C. Gourdon, Towards the design of an intensified coagulator, *Chem. Eng. Process. Process Intensif.* 121 (2017) 1–14, <https://doi.org/10.1016/j.cep.2017.08.003>.
- [61] J.Z. Fang, D.J. Lee, Micromixing efficiency in static mixer, *Chem. Eng. Sci.* 56 (2001) 3797–3802.
- [62] L. Falk, J.-M. Commenge, Performance comparison of micromixers, *Chem. Eng. Sci.* 65 (2010) 405–411, <https://doi.org/10.1016/j.ces.2009.05.045>.